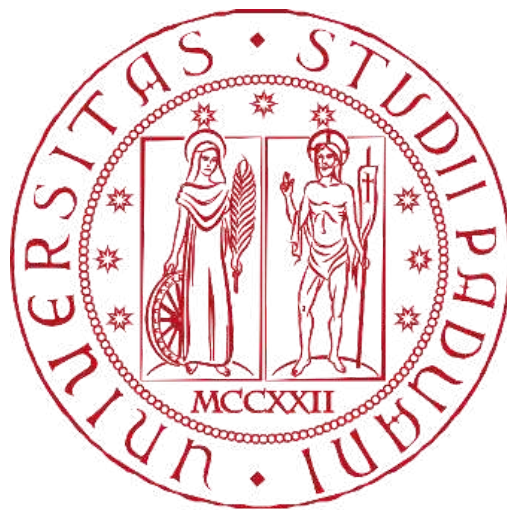


University of Padua

School of Medicine and Surgery

Master's Degree Programme in Medical Biotechnologies

Department of Molecular Medicine



OPTIMIZATION OF LENTIVIRAL TRANSDUCTION FOR EBOLA
VP40 EXPRESSION IN A HARD-TO-TRANSDUCE HUMAN CELL
LINE

Supervisor: Prof.ssa Maria Cristina Parolin

Co-Supervisor: Professor Robert Davey

Student: Marco Petralia

Academic year: 2024/2025

I. INTRODUCTION

1. Ebola Virus: Biology, Structure, and Pathogenesis
 - 1.1. The EBOV Replication Cycle
 - 1.2. Pathogenesis and Immune Evasion
2. Biosafety Constraints and the Limitation of Current BSL-2 Approaches
3. Experimental Models for EBOV Research
 - 3.1. Cellular Models
 - 3.2. Surrogate Viral Systems
 - 3.3. In Vivo Models
4. Remaining Gaps in Current BSL-2 VP40-Based Systems
5. VP40 as a Minimal Driver of Assembly and Budding
6. Lentiviral Delivery as a Controlled VP40 Expression Strategy
7. Rationale for Using Huh-7 Cells and Their Limitations
8. Aim of This Study

II. MATERIALS AND METHODS

1. Cell Lines and Culture Conditions
2. Plasmids, Vector Design, and Construction
 - 2.1. Lentiviral System Overview and Source Materials
 - 2.2. Primer Design and Cloning Strategy
 - 2.3. PCR Amplification and Purification
 - 2.4. HiFi Assembly
 - 2.5. Transformation, Screening, and Quality Control
3. Lentiviral Particle Production and Functional Titration
 - 3.1. Production of Pseudotyped Lentiviral Particles
 - 3.2. Functional Titration of Pseudotyped Lentiviral Particles

4. Transduction of Target Cell Lines
5. Assessment of Transduction-Associated Cytotoxicity
6. Selection of Stably Transduced Cells
7. Western Blotting
 - 7.1. Densitometry and Data Analysis

III. RESULTS

1. Confirmation of VP40-FLAG Construct Generation
2. Preliminary Expression Check by Transient Transfection
3. Production and Titration of Pseudotyped Lentiviral Particles
4. Optimization of Lentiviral Production and Target Cell Transduction
5. Cell Viability Following Lentiviral Transduction
 - 5.1. HEK293T Cells
 - 5.2. Huh-7 Cells
6. Expression of GFP and VP40-FLAG Assessed by Western Blotting
 - 6.1. Comparison Between HEK293T and Huh-7 Cells
 - 6.2. MOI-Dependent VP40-FLAG Expression in Huh-7 Cells
7. Generation of Stably Transduced Huh-7 Cells
8. Qualitative Assessment of Transduction Efficiency by Confocal Microscopy

IV. DISCUSSION

1. Overall Significance and the Necessity of Physiologically Relevant BSL-2 Platforms
2. Optimization of Lentiviral Production and Delivery
3. Balancing Reductionism and Biological Relevance
4. Cell-Type Dependence and Functional Consequences
5. Confocal Microscopy as Qualitative Validation of Delivery Fidelity
6. Limitations of This Study

V. CONCLUSIONS

1. Synthesis of Findings and Validation of the Platform
2. Quantitative Fidelity and Stoichiometric Control
3. Highlighting Achievements and Reconciling Limitations
4. The Bioenergetic Cost of Transduction
5. Future Directions

VI. REFERENCES

I. INTRODUCTION

1. Ebola Virus: Biology, Structure, and Pathogenesis.

Ebola virus (EBOV) is a filamentous, enveloped, negative-sense RNA virus of the *Filoviridae* family. EBOV virions are pleomorphic, typically ~80 nm in diameter and up to several micrometres in length, and contain a ~19 kb genome encoding seven structural proteins: NP, VP35, VP40, GP, VP30, VP24, and L. The virion consists of a host-derived lipid envelope bearing trimeric glycoprotein (GP) spikes, a matrix layer composed predominantly of VP40 and the minor matrix protein VP24, and an internal ribonucleoprotein (RNP) complex in which genomic RNA is encapsidated by NP and associated with VP35, VP30 and the L polymerase. Among these components, the matrix protein VP40 is particularly critical, serving not only as a structural scaffold but also as a dynamic regulator of the viral life cycle.

1.1 The EBOV replication cycle proceeds through tightly regulated stages:

- **Attachment and Entry:** The replication cycle begins with the attachment of the viral GP to cell-surface attachment factors, such as C-type lectins (e.g., DC-SIGN) or phosphatidylserine receptors (e.g., TIM-1, AXL) [12, 18]. Following attachment, virions are internalized via macropinocytosis, a non-specific endocytic pathway triggered by viral signaling.
- **Fusion:** Within the acidifying late endosome, host proteases (Cathepsins B and L) cleave the viral GP, exposing the receptor-binding domain. This primed GP interacts with the intracellular receptor Niemann-Pick C1 (NPC1), a critical step that triggers fusion between the viral envelope and the endosomal membrane, releasing the nucleocapsid into the cytoplasm [5, 18].
- **Transcription and Replication:** Upon uncoating, the RNP complex initiates primary transcription. The viral polymerase (L), with VP35 as a cofactor and VP30 as a transcriptional activator, synthesizes monocistronic, capped, and polyadenylated mRNAs [11, 16]. As viral protein levels rise, the polymerase switches from transcription to genome replication, synthesizing a full-length positive-sense antigenome (cRNA) which serves as a template for new negative-sense genomic RNA (vRNA) [16]. This process occurs within distinct cytoplasmic inclusion bodies, which concentrate viral components and shield them from innate immune detection [14].
- **Assembly and Egress:** The late stage of infection is orchestrated by VP40. Newly synthesized VP40 is trafficked to the plasma membrane, a process dependent on the host COPII transport machinery [7]. At the plasma membrane inner leaflet, VP40 dimers bind anionic lipids, specifically phosphatidylserine (PS) and phosphatidylinositol 4,5-bisphosphate (PI(4,5)P₂) [3, 13]. This electrostatic interaction triggers a conformational change, inducing VP40 oligomerization into hexameric lattices that drive

membrane curvature [5]. These lattices recruit the nucleocapsid and GP to budding sites. Finally, VP40 utilizes "late domain" motifs (PTAP and PPxY) to recruit host ESCRT machinery (e.g., Tsg101, Nedd4), which mediates the membrane scission event required to release filamentous virions [1, 8].

EBOV infection results in severe multisystem disease. Viral replication in monocytes, macrophages, dendritic cells, hepatocytes, and endothelial cells leads to innate immune suppression, excessive inflammatory cytokine release, coagulopathy, vascular leakage, and multiorgan failure. Notably, VP40 contributes to pathogenesis beyond its role in virion assembly; it can be packaged into host-derived exosomes, which, upon delivery to immune cells, can induce bystander apoptosis and contribute to the profound lymphopenia characteristic of Ebola virus disease [8]. Although therapeutic options remain limited, approved countermeasures include the rVSV-ZEBOV (Ervebo) vaccine and monoclonal antibody treatments (Inmazeb, Ebanga) [4], which are primarily effective against the *Zaire ebolavirus* species. Outbreaks continue to occur unpredictably and that viral evolution poses risk to vaccine-only strategies. This highlights the critical need for broad-spectrum antivirals. Promising targets include the highly conserved VP40 protein, for which potential small-molecule inhibitors have been identified through computational drug discovery (CADD) screens. However, detailed mechanistic study and screening of such late-stage assembly targets are severely constrained by the requirement for maximum biosafety containment.

2. Biosafety Constraints and the Limitation of Current BSL-2 Approaches

The BSL-4 Bottleneck Research on the full life cycle of Ebola virus (EBOV) is strictly confined to Biosafety Level 4 (BSL-4) facilities. These high-containment laboratories are scarce, technologically complex, and prohibitively expensive to operate [1, 2]. Beyond financial costs, the operational constraints—such as the requirement for positive-pressure suits and rigorous decontamination protocols—severely limit experimental throughput [11]. This creates a fundamental bottleneck in EBOV research, particularly for large-scale small-molecule screening and detailed mechanistic studies that require high-resolution imaging or complex genetic manipulation. Consequently, the development of broad-spectrum therapeutics has been slowed by the inability to easily access the pathogen for routine experimentation.

The Limitations of Plasmid-Based Surrogates: To circumvent these barriers, "life-cycle modeling" under BSL-2 conditions has become the standard approach. While effective, the majority of these systems rely on the transient transfection of plasmids driven by strong constitutive promoters (e.g., CMV or CAG) to express viral proteins [2, 11]. While this method successfully generates viral components, it introduces significant biological artifacts. Transient transfection typically results in a "burst" of supraphysiological protein expression that bypasses the intricate temporal regulation of a natural infection. In an authentic EBOV infection, proteins like VP40 are synthesized in a tightly controlled stoichiometric ratio relative to other viral components (e.g., NP and GP) [16]. Disrupting this stoichiometry can force interactions that do

not occur physiologically, mask the effects of restriction factors, or overwhelm cellular trafficking pathways (e.g., the ESCRT or COPII machinery) [3, 5]. Therefore, there is an urgent need for BSL-2 platforms that move beyond simple overexpression to offer stable, tunable control of viral protein levels.

3. Experimental Models for EBOV Research

To deconstruct EBOV biology without the risks of handling live virus, a diverse toolkit of surrogate systems has been developed. These models range from simplified cell culture systems to complex *ex vivo* tissues, each offering a trade-off between manipulability and physiological relevance.

3.1. Cellular Models

- **Immortalized Cell Lines:** Standard human cell lines remain the workhorse of filovirus research. HEK293T cells are widely utilized due to their high permissiveness to transfection and viral entry; however, they lack the specific innate immune and metabolic profiles of natural EBOV targets [2]. In contrast, Hepatocellular carcinoma cells (Huh-7) represent a more relevant model given the liver's central role in EBOV pathogenesis, though they are notoriously more difficult to transduce [1, 19].
- **Primary Cells and Explants:** To bridge the gap between cell lines and host organisms, recent studies have utilized human skin explants. These models preserve the 3D tissue architecture and allow for the study of viral translocation across epidermal layers, offering insights into transmission dynamics that monolayer cultures cannot provide [10].

3.2. Surrogate Viral Systems

- **Virus-Like Particles (VLPs):** Expression of the matrix protein VP40, alone or in combination with GP and NP, results in the budding of filamentous particles that morphologically mimic the authentic virus. VLP systems are the "gold standard" for studying the mechanics of viral assembly and egress (budding) in a safe BSL-2 environment [1, 2].
- **Minigenome Systems:** These systems model the replication and transcription machinery. They utilize a distinct viral RNA analog containing a reporter gene (e.g., Luciferase) flanked by EBOV non-coding leader and trailer sequences. When supplied with the viral RNP proteins (NP, VP35, VP30, L), the minigenome is recognized and replicated, allowing for the screening of polymerase inhibitors [11].
- **Transcription- and Replication-Competent VLPs (trVLPs):** This hybrid system packages a minigenome into a VLP. Unlike standard VLPs, trVLPs can infect target cells and undergo a single round of replication [1, 11]. This makes them powerful tools for

studying viral entry and primary transcription, although they still rely on helper plasmids to provide structural proteins for subsequent rounds of infection.

3.3. In Vivo Models Animal models remain essential for vaccine and pathogenesis studies. Non-human primates (NHPs) best recapitulate the severe hemorrhagic fever seen in humans but are ethically complex and restricted to BSL-4 [4]. Small animal models, such as mice, require the virus to be "adapted" (e.g., via mutations in VP40 or NP) to overcome host restriction factors like Tetherin, which can sometimes alter the viral biology compared to the wild-type human pathogen [8].

4. Remaining Gaps in Current BSL-2 VP40-Based Systems

The Artifacts of Supraphysiological Expression

Despite the utility of minigenome, VLP, and trVLP systems, current BSL-2 platforms suffer from a fundamental limitation: the reliance on transient plasmid transfection driven by strong, constitutive promoters (e.g., CMV, CAG) [1]. In a natural EBOV infection, viral protein synthesis is temporally regulated; NP and VP35 accumulate early to drive replication, while VP40 expression is delayed to prevent premature assembly [16]. Plasmid transfection bypasses this regulation, resulting in an immediate, "burst-like" accumulation of VP40 to supraphysiological levels. This stoichiometric imbalance can mask key regulatory features of the virus. For instance, excessive VP40 concentrations can artificially override the requirement for specific host trafficking factors, such as the COPII transport machinery (Sec24C), by saturating the pathway or forcing non-canonical transport routes that do not reflect authentic infection [7]. Furthermore, uncontrolled expression can induce cellular stress responses (e.g., the Unfolded Protein Response) that confound the interpretation of cytotoxicity and assembly kinetics [17].

The "Conformational Switch" and Oligomeric Regulation

The lack of quantitative control in current models specifically hinders the study of VP40's structural plasticity. VP40 is a "transformer" protein that assumes distinct oligomeric states depending on its local concentration and cellular localization [15]. In the cytoplasm, it exists as a dimer or an RNA-binding octamer, the latter of which is implicated in the negative regulation of viral transcription [16]. At the plasma membrane, it rearranges into hexamers and extensive filamentous lattices to drive budding [3, 5]. The transition between these states is likely concentration-dependent. Current overexpression models, which flood the cytoplasm with protein, effectively lock VP40 into its assembly-competent state, preventing the exploration of the delicate equilibrium between the transcriptional-regulatory octamer and the budding-active hexamer [15]. Consequently, the relationship between these dual functions remains largely unresolved in a BSL-2 context.

Limitations in Antiviral Screening and Host Factor Analysis

Finally, the inability to tune protein levels limits the utility of these systems for translational research. High-throughput screening (HTS) for budding inhibitors requires a system where the target protein (VP40) is present at physiological levels; gross overexpression can artificially increase the drug concentration required for inhibition (IC₅₀), leading to false negatives [6]. Additionally, the efficiency of VP40 budding is intrinsically linked to the host cell environment, varying sharply due to differences in plasma membrane lipid composition (e.g., PI(4,5)P₂ levels) and the presence of restriction factors like Tetherin (BST-2) [8, 13]. Existing plasmid-based platforms often overwhelm these host restrictions, masking subtle virus-host interactions that could serve as therapeutic targets. Collectively, these gaps highlight the critical need for a tunable, stable delivery system that allows for quantitative VP40 expression to dissect matrix-driven assembly with greater physiological relevance [1, 2].

5. VP40 as a Minimal Driver of Assembly and Budding

Structural and Functional Versatility

The viral matrix protein VP40 (~40 kDa) serves as the primary driver of Ebola virus assembly and egress. It is the most abundant protein in the virion and is sufficient, in the absence of any other viral components, to induce the formation and release of filamentous Virus-Like Particles (VLPs) that are morphologically indistinguishable from the authentic pathogen [2, 3]. This autonomous budding capability stems from VP40's ability to coordinate a complex series of protein-lipid and protein-protein interactions at the plasma membrane. Structurally, VP40 is composed of distinct N-terminal and C-terminal domains connected by a flexible linker [15]. This architecture allows the protein to undergo drastic conformational changes, shifting from a dimeric state during transport to extensive hexameric lattices upon membrane association [5].

Mechanism of Membrane Scission and Egress

The budding process is initiated when VP40 engages anionic lipids, specifically phosphatidylserine (PS) and phosphatidylinositol 4,5-bisphosphate (PI(4,5)P₂), at the inner leaflet of the plasma membrane [3, 13]. These electrostatic interactions are critical; mutations that disrupt the basic patches in VP40's C-terminal domain abolish membrane binding and subsequent particle release [3, 13]. Once the matrix lattice is established, inducing membrane curvature, VP40 recruits the host's cellular machinery to execute the final fission step. Through its conserved Late Domain (L-domain) motifs—specifically the PTAP and PPxY sequences at the N-terminus—VP40 interacts with the host ESCRT (Endosomal Sorting Complex Required for Transport) machinery (e.g., Tsg101) and ubiquitin ligases (e.g., Nedd4), respectively [8, 15]. This recruitment hijacks the host's membrane scission apparatus to sever the budding virion from the cell surface. Because VP40 is highly conserved across all Ebolavirus species and is essential for viral dissemination, it represents a high-value target for broad-spectrum antiviral development [4, 6].

6. Lentiviral Delivery as a Controlled VP40 Expression Strategy

Overcoming the Limitations of Transfection

Given the stoichiometric sensitivity of VP40 assembly, lentiviral vectors offer a distinct methodological advantage over traditional plasmid transfection. Lentiviral transduction mediates the stable integration of the transgene into the host genome, ensuring consistent, long-term expression without the extreme fluctuations associated with transient episomal vectors [2]. Unlike transfection reagents (e.g., lipofection), which often exhibit high toxicity and low efficiency in primary or disease-relevant cells (such as hepatocytes), vesicular stomatitis virus G-protein (VSV-G) pseudotyped lentiviruses possess a broad tropism and can efficiently transduce "hard-to-transfect" cell lines like Huh-7 [1].

Tunability and Physiological Relevance

Crucially, lentiviral delivery transforms VP40 expression from a binary variable (present/absent) into a tunable quantitative parameter. By modulating the Multiplicity of Infection (MOI), the copy number of the integrated provirus can be titrated to achieve protein levels that mirror the progressive accumulation seen during natural infection, rather than the immediate saturation caused by plasmids [16]. This control is essential for dissecting concentration-dependent phenomena, such as the switch between VP40's transcriptional regulatory function (octamers) and its matrix-forming function (hexamers) [5]. Furthermore, this platform enables the standardized interrogation of host restriction factors (e.g., Tetherin) in a uniform genetic background, facilitating the screening of VP40-targeting antivirals under standardized, reproducible conditions [6, 8]. Despite these clear advantages, lentiviral approaches for EBOV assembly research remain underdeveloped compared to convenient but artifact-prone plasmid systems.

7. Rationale for Using Huh-7 Cells and Their Limitations

The Physiological Relevance of the Hepatic Model

While HEK293T cells are the industry standard for viral vector production and basic expression studies, their utility in modeling authentic pathogen-host interactions is limited. As an embryonic kidney line transformed with Adenovirus and SV40 viral oncogenes, HEK293T cells are engineered for maximal protein yield rather than physiological fidelity; they lack the specific metabolic and innate immune competence of somatic target cells [2].

In contrast, the Huh-7 hepatoma cell line represents a biologically superior model for Ebolavirus research. In clinical cases of Ebola Virus Disease (EVD), the liver is a primary site of robust viral replication, and severe hepatocellular necrosis is a hallmark of fatal outcomes, contributing directly to coagulopathy and systemic failure [17, 19]. Huh-7 cells retain key hepatocyte-specific characteristics, including lipid metabolic pathways that regulate the composition of the plasma membrane [13]. Since VP40 matrix assembly is strictly dependent on specific anionic lipids (Phosphatidylserine and PI(4,5)P2) and hijacks the host COPII vesicular transport system for

trafficking, the hepatocyte intracellular environment provides a more authentic context for studying these molecular events than non-target kidney cells [7, 13]. Furthermore, Huh-7 cells have been successfully employed to establish trVLP systems that model the complete viral life cycle, validating their permissiveness to filoviral replication [1].

Technical Challenges and Limitations

Despite their biological advantages, Huh-7 cells present significant technical hurdles that this study aims to address. Unlike HEK293T cells, which have defective innate immune sensing pathways (facilitating high plasmid uptake), Huh-7 cells possess more competent pattern recognition receptors (PRRs), including RIG-I [16, 20]. Consequently, they mount a stronger antiviral response upon exposure to exogenous nucleic acids or viral vectors, rendering them "hard-to-transduce" and significantly lowering transgene expression efficiency [1].

Additionally, the strong constitutive promoters typically used in expression vectors (such as CMV) often show reduced activity in differentiated hepatocytes compared to the supraphysiological activity seen in HEK293T cells. Finally, while they model the hepatic aspect of the disease, Huh-7 cells do not recapitulate the endothelial dysfunction or the complex immunological signaling of the myeloid compartment (macrophages/dendritic cells), which are the initial targets of infection [10, 19]. These constraints necessitate the stringent optimization of transduction protocols (e.g., polycations, spinoculation) to overcome the cellular entry barriers and achieve detectable, physiologically relevant VP40 levels.

8. Aim of This Study

Contextual Rationale: As detailed in the preceding sections, the matrix protein VP40 is the fundamental driver of Ebolavirus assembly and egress [3]. However, current BSL-2 experimental models relying on plasmid transfection fail to recapitulate the precise stoichiometric and temporal regulation of natural infection, often resulting in overexpression artifacts that mask subtle host-pathogen interactions [5, 16]. Furthermore, while the liver is a primary target of EBOV pathogenesis [19], research is hampered by the technical difficulty of delivering genetic material into biologically relevant hepatocyte models like Huh-7, which possess active innate immune barriers [1].

Primary Objective: To bridge the gap between artifact-prone overexpression systems and restricted BSL-4 infection models, the primary aim of this thesis is to design, optimize, and validate a lentiviral delivery platform for EBOV VP40. By leveraging the stable integration and controllable kinetics of lentiviral transduction [6], this study seeks to create a reproducible BSL-2 model capable of expressing VP40 in "hard-to-transduce" human hepatocytes.

Specific Goals: To achieve this aim, the study is structured around three core objectives:

1. **Construction of a Biosafety-Compliant Transfer Vector:** To generate a third-generation lentiviral transfer vector encoding VP40 fused to a FLAG tag. This involves adapting the coding sequence from a donor plasmid into a lentiviral backbone that retains the CMV promoter for robust expression while ensuring safety via a split-genome packaging strategy.
2. **Optimization of Transduction in Restrictive Hosts:** To systematically overcome the entry barriers of Huh-7 cells. This involves establishing an optimized transduction protocol by titrating chemical adjuvants (Polybrene) and employing physical enhancement methods (spinoculation) to maximize delivery efficiency without inducing cell death, thereby addressing the limitations cited in current literature regarding hepatocyte transduction [1].
3. **Validation of Tunable Expression:** To demonstrate that the established system allows for controlled, dose-dependent protein expression. By correlating Multiplicity of Infection (MOI) with protein levels (via Western Blot and Confocal Microscopy), this study aims to validate the platform's utility for future stoichiometric studies and its potential as a scalable tool for screening VP40-targeting antivirals [6].

II. MATERIALS AND METHODS

This chapter describes plasmid construction, bacterial transformation, lentiviral production and titration, transduction optimization in Huh-7 cells and downstream validation assays (western blot and confocal microscopy).

1. Cell Lines and Culture Conditions

HEK293T , and Huh-7 cells were maintained under standard culture conditions at 37 °C with 5% CO₂. HEK293T and Huh-7 cells were grown in Dulbecco's Modified Eagle Medium (DMEM, high glucose) supplemented with 10% fetal bovine serum (FBS), 1% penicillin–streptomycin (P/S), and L-glutamine. Cells were routinely monitored for mycoplasma contamination and passaged at 70–80% confluence using 0.05% trypsin–EDTA.

2. Plasmids, Vector Design, and Construction

2.1. Lentiviral System Overview and Source Materials

The expression system employed in this study is a third-generation lentiviral packaging system designed to maximize biosafety by splitting the viral components across four separate plasmids. The system comprises:

- Packaging Vectors: pLP1 (~6.9 kb) encoding the HIV-1 structural protein Gag and enzymatic protein Pol; pLP2 (~4.2 kb) encoding the regulatory protein Rev; and pLP/VSV-G (~5.8 kb) encoding the Vesicular Stomatitis Virus G glycoprotein, which provides the envelope protein essential for broad tropism.
- Transfer Vector: pEGFP (~7.7 kb) served as the backbone for cloning. It contains a truncated 5' LTR, a packaging signal (Ψ), and a 3' LTR (Δ U3) for self-inactivation. Crucially, it retains a strong constitutive CMV promoter to drive transgene expression and a Blasticidin S Deaminase (BSD) gene for antibiotic selection, enabling the generation of stable cell lines.
- Insert Source: The coding sequence for Ebola virus VP40 fused to a FLAG tag (VP40-FLAG) was sourced from the donor plasmid pcDNA3.1+EBOV-FLAG-VP40.

Packaging Plasmids & Transfer Vector

- pLP1 (rev) (~ 6.9 kb)
RSV Promoter – Rev – β -globin Poly(a)
- pLP2 (gag/pol) (~ 4.2 kb)
CMV Promoter – HIV Gag/Pol – RRE – β -globin Poly(A)
- pVSV-G (~ 5.8 kb)
CMV Promoter – VSV-G – β -globin Poly(A)
- pEGFP (~ 7.7 kb) Transfer Vector Backbone
5' LTR – HIV-1 Ψ – RRE – CMV Promoter – **EGFP** – BSD – 3' LTR
- pcDNA3.1+EBOV-FLAG-VP40 (~ 6.3 kb) VP40-FLAG insert
5' LTR – HIV-1 Ψ – RRE – CMV Promoter – **VP40+FLAG** – BSD – 3' LTR

Figure 1. Plasmid Maps of the Third-Generation Lentiviral Packaging System.

The packaging system consists of three helper plasmids and one transfer vector. *pLP1* (~ 6.9 kb) encodes the HIV-1 structural protein Gag and the enzymatic protein Pol. *pLP2* (~ 4.2 kb) encodes the regulatory protein Rev. *pVSV-G* (~ 5.8 kb) encodes the Vesicular Stomatitis Virus G glycoprotein, which provides the envelope protein essential for broad tropism and pseudotyping. *pEGFP* (~ 7.7 kb) is the transfer vector backbone, containing the Blasticidin S Deaminase (BSD) selection marker.

2.2. Primer Design and Cloning Strategy



To generate the pVP40-FLAG transfer vector, a homology-directed cloning strategy (NEBuilder HiFi DNA Assembly) was designed. Two primer pairs were engineered using NEBuilder guidelines to generate 15–25 bp overlapping homology arms required for efficient recombination:

1. Backbone Primers: Designed to amplify the pEGFP vector while deleting the GFP coding sequence.
2. Insert Primers: Designed to amplify the VP40-FLAG coding sequence with 5' extensions homologous to the linearized backbone ends.

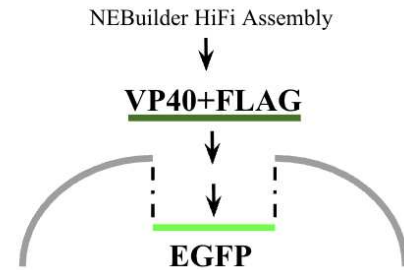
All primers were designed with matched melting temperatures ($\geq 60^\circ\text{C}$) to ensure specific annealing during high-fidelity amplification. Note that this step required iterative optimization; two rounds of primer redesign were necessary to ensure correct fragment orientation and sufficient homology for efficient assembly.

HiFi Assembly Strategy for Generation of the pVP40-FLAG Transfer Vector

Panel A: The Source Material

- pEGFP Backbone

- VP40-FLAG Insert


Panel B: The Source Material



Panel C: The Final Construct (pVP40-FLAG)



Figure 2. HiFi Assembly Strategy for Generation of the pVP40-FLAG Transfer Vector.

The VP40-FLAG coding sequence, sourced from the pcDNA3.1 donor plasmid (left, ~1.1 kb insert size), was cloned into the pEGFP transfer vector backbone (middle, ~6.9 kb). The final resulting plasmid (pVP40-FLAG transfer vector) maintains the BSD selection marker.

2.3. PCR Amplification and Purification

PCR reactions were performed using Q5 High-Fidelity 2X Master Mix (New England Biolabs) to minimize replication errors. A critical optimization step involved the adjustment of extension times to match the fragment sizes: 30 seconds for the VP40-FLAG insert (~1.1 kb) and 6–7 minutes for the vector backbone (~6.9 kb).

Following amplification, 1 μ L of DpnI restriction enzyme was added directly to each reaction and incubated to selectively digest the methylated parental plasmid templates, thereby reducing the background of non-recombinant colonies. PCR products were resolved on a 1% agarose gel. Bands corresponding to the linearized backbone and insert were excised and purified using a silica-based Gel Extraction Kit to remove non-specific amplicons and primer dimers.

2.4. HiFi Assembly

The purified backbone and insert fragments were assembled using the NEBuilder HiFi DNA Assembly Master Mix. To maximize assembly efficiency, a molar ratio of 2:1 (Insert:Vector) was utilized in a total reaction volume of 10 μ L. The reaction was incubated at 50°C for 15–60 minutes to allow for 5' exonuclease recession, annealing of complementary overlaps, and ligase-mediated sealing of the nicks.

2.5. Transformation, Screening, and Quality Control

The assembly reaction mixture (1–2 μ L) was transformed into NEB Stable Competent *E. coli* via heat shock (42°C, 30 s). This specific bacterial strain was selected to maintain the stability of the lentiviral Long Terminal Repeats (LTRs), which are prone to recombination in standard strains. Cells were recovered in NEB Outgrowth Medium for 60 minutes at 30°C and plated on LB-agar containing Ampicillin or Carbenicillin.

Initial transformation efficiency was low, necessitating the optimization of PCR extension times and the stringent screening of multiple colonies. Two to six well-isolated colonies were picked and screened by overnight culture in LB-Ampicillin, followed by plasmid isolation (Miniprep). Positive clones were definitively confirmed by Sanger sequencing covering the cloning junctions and the full VP40 ORF. A validated high-fidelity clone was subsequently expanded to 50 μ L LB-Ampicillin culture for Maxiprep purification to generate the high-quality plasmid stock required for downstream viral production.

3. Lentiviral Particle Production and Functional Titration

3.1 Production of Pseudotyped Lentiviral Particles

Lentiviral particles pseudotyped with the VSV-G envelope were generated by transient co-transfection of HEK293T producer cells. This cell line was selected for its high transfectability and capacity for high-titer viral production. The third-generation packaging system was employed to ensure biosafety, utilizing four plasmids: pLP1 (expressing *gag/pol*), pLP2 (expressing *rev*), pLP/VSV-G (expressing the envelope glycoprotein), and either the pEGFP control or the pVP40-FLAG transfer vector. Transfections were performed using the lipid-based TransIT-LT1 reagent (Mirus Bio), which was selected after preliminary optimization showed superior transfection efficiency and reduced cytotoxicity compared to the calcium phosphate (CaCl) precipitation method. Briefly, HEK293T cells were seeded to achieve 70–80% confluence on the day of transfection. The plasmid DNA mixture was prepared at a standard mass ratio of 4:2:1:4 μ g (Transfer:pLP1:pLP2:VSV-G) to optimize the stoichiometry of viral component expression. The DNA lipid complexes were formed by incubating the plasmids with LT1 reagent in Opti-MEM (Gibco) for 20 minutes at room temperature before being added dropwise to the producer cells. Viral supernatants containing the pseudotyped lentiviral particles were harvested at 48 hours post-transfection. To remove cell debris, supernatants were clarified by low-speed centrifugation (500 x g, 5 min) then aliquoted and stored at -80°C to preserve infectivity.

3.2 Functional Titration of Pseudotyped Lentiviral Particles

To determine the concentration of infectious virions, functional titration was performed using a GFP-based transduction assay. Unlike physical titration methods (e.g., p24 ELISA) which detect both infectious and non-infectious particles, this method specifically quantifies Transducing Units per milliliter (TU/mL), providing a functional measure of viral infectivity. HEK293T cells were used as the indicator cell line due to their high permissiveness to VSV-G pseudotyped

vectors. Cells were seeded in 96-well plates at a density of $2.5 - 3.0 \times 10^4$ cells/well in 100 μ L of complete medium. The following day, viral stocks were thawed on ice, and 10-fold serial dilutions (ranging from 10^{-1} to 10^{-5}) were prepared in serum-free medium. Transduction was initiated by removing the culture medium and adding 30 μ L of each viral dilution to the wells in the presence of polybrene (8 μ g/mL) to neutralize electrostatic repulsion. To enhance viral entry, plates were subjected to spinoculation (2000 x g, 2 hours, 25°C). Following centrifugation, cells were incubated for 4-6 hours at 37°C, after which 170 μ L of fresh complete medium was added to dilute the polybrene and bring the final volume to 200 μ L per well. At 72 hours post-transduction, cells were analyzed by fluorescence microscopy. Wells exhibiting discrete, countable GFP-positive colonies (typically in the range of 5–20% transduction efficiency) were selected for quantification to ensure the assay remained within the linear range and to minimize the probability of multiple viral integrations per cell (Poisson distribution).

The functional titer was calculated using the following formula:

$$\text{Titer (TU/mL)} = (\text{Number of GFP}^+ \text{ Colonies} \times \text{Dilution Factor}) / \text{Volume of Virus Added (mL)}.$$

Using a viral inoculum volume of 30 μ L (0.03mL), the calculation was derived as:

$$\text{TU/mL} = (\text{GFP Count}) \times (\text{Dilution Factor}) \times 33.3$$

Based on this protocol, high-quality viral preparations yielded functional titers of approximately 2×10^6 , TU/mL. These calculated titers were subsequently used to determine the precise volume of viral supernatant required to achieve specific Multiplicities of Infection (MOI) for downstream experiments in Huh-7 cells.

4. Transduction of Target Cell Lines

To ensure reproducible infection rates, Huh-7 and HEK293T target cells were seeded 24 hours prior to transduction in 6-well or 12-well plates to achieve a confluence of 60–70% at the time of infection ($2.5 - 5.0 \times 10^5$ cells/well). Viral inocula were prepared by diluting the concentrated lentiviral stocks in fresh complete medium to achieve specific Multiplicities of Infection (MOI) ranging from 0.25 to 1.0. To overcome the electrostatic repulsion between the viral envelope and the cell membrane—a known barrier in restrictive cell lines like Huh-7—polybrene was added to the transduction medium. A concentration gradient (2, 5, and 8 μ g/mL) was tested to determine the optimal balance between entry efficiency and cytotoxicity. In selected optimization experiments, spinoculation was applied: plates were centrifuged at 2300 x g for 60 minutes at 20°C immediately after viral addition to mechanically sediment viral particles onto the cell surface. Following infection (or spinoculation), cells were incubated for 6 hours at 37°C before the viral medium was replaced with fresh complete DMEM to minimize toxic effects from the polycation. Cells were subsequently cultured for 48–72 hours prior to protein harvesting or microscopic analysis.

5. Assessment of Transduction-Associated Cytotoxicity

Given the sensitivity of Huh-7 cells to chemical adjuvants and viral load, cell viability was rigorously monitored at 24, 48, and 72 hours post-transduction. Quantitative evaluation was performed using the Trypan Blue dye exclusion method. Briefly, cells were harvested by trypsinization, stained with 0.4% Trypan Blue solution (1:1 v/v), and counted using a hemocytometer. Viability was expressed as a percentage relative to mock-transduced controls (cells treated with polybrene but without virus).

Qualitative assessment was also performed via brightfield microscopy to monitor morphological changes indicative of cytopathic effects (CPE), such as cell rounding, vacuolization, or detachment.

- Mild Conditions (Low MOI/Polybrene): Viability remained comparable to controls (>90%), with cell densities reaching $\sim 2\text{--}3 \times 10^6$ cells/mL at endpoint.
- Harsh Conditions (High MOI/Polybrene): Transduction with MOI > 1.0 or polybrene >8 $\mu\text{g}/\text{mL}$ resulted in significant cytotoxicity, characterized by a marked reduction in viable cell density ($\sim 4 \times 10^5$ cells/mL) and widespread cell death. Based on these "viability screens," an upper limit of MOI 1.0 was established for all subsequent functional assays to ensure that observed phenotypes were due to viral protein expression rather than cellular stress.

6. Selection of Stably Transduced Cells

To generate stable cell lines constitutively expressing GFP or VP40-FLAG, the established transduction protocol (MOI 0.5, 2 $\mu\text{g}/\text{mL}$ polybrene, spinoculation) was followed by antibiotic selection. Prior to selection, a Blasticidin kill-curve was generated to determine the minimum concentration required to kill 100% of non-transduced Huh-7 cells. Cells were seeded at 50% confluence and treated with increasing concentrations of Blasticidin S (2–15 $\mu\text{g}/\text{mL}$). Media was refreshed every 3 days. Complete cell death of non-transduced controls was observed between 5 and 10 $\mu\text{g}/\text{mL}$ within 7–10 days.

Consequently, a working concentration of 6 $\mu\text{g}/\text{mL}$ was selected. Transduced populations were subjected to selection 48 hours post-infection. The selective medium was refreshed every 2–3 days to remove dead cells and maintain selective pressure. Selection was continued for approximately 14 days until a homogeneous, drug-resistant population of colonies was obtained. These stable pools were expanded, cryopreserved, and validated for transgene expression via Western Blot and fluorescence microscopy.

7. Western Blotting

Cells were washed twice with ice-cold PBS and lysed in RIPA buffer (50 mM Tris-HCl pH 7.4, 150 mM NaCl, 1% NP-40, 0.5% Sodium Deoxycholate, 0.1% SDS) supplemented with a Protease Inhibitor Cocktail (e.g., PMSF/Aprotinin) to prevent protein degradation. Lysates were clarified by centrifugation (14,000 x g, 15 min, 4°C), and total protein concentration was determined using the BCA Protein Assay Kit (Pierce).

Samples (20–30µg of total protein) were denatured at 95°C for 5 minutes in the Laemmli sample buffer and resolved on 10–12% SDS-PAGE gels. Proteins were electro-transferred onto PVDF membranes (activated in methanol) using a wet transfer system. Membranes were blocked for 1 hour at room temperature in 5% non-fat dry milk in TBST (Tris-buffered saline with 0.1% Tween-20).

7.1. Densitometry and Data Analysis

Quantitative analysis of protein expression was performed using ImageJ software (NIH). Band intensities for VP40-FLAG and GFP were measured and normalized to the corresponding GAPDH loading control to account for variations in sample loading.

Statistical analysis was performed using Excel. Differences between groups (e.g., HEK293T vs. Huh-7 expression levels) were evaluated using an unpaired Student's t-test. Results are presented as mean \pm Standard Deviation (SD) from at least three independent biological replicates (n=3). Statistical significance is indicated where $p < 0.05$.

III. RESULTS

1. Confirmation of VP40-FLAG Construct Generation

Correct cloning of the VP40-FLAG expression construct into the lentiviral backbone was confirmed prior to viral production. PCR amplification produced fragments of the expected size for both the linearized vector and the VP40 insert. Colony PCR screening of transformed *E. coli* yielded positive clones containing the assembled construct. Sanger sequencing verified correct integration and orientation of the VP40-FLAG insert. These steps established the final plasmid used for subsequent lentiviral production.

2. Preliminary Expression Check by Transient Transfection

Following confirmation of the sequence fidelity, the newly constructed pVP40-FLAG transfer vector was functionally tested by transient transfection into HEK293T cells. Transfection efficiency, visualized by co-transfection of pEGFP, was consistently high (~ 80%) across replicates. Western blot analysis of cell lysates collected 48 hours post-transfection confirmed the robust expression of the VP40-FLAG protein (~ 40 kDa) using an anti-FLAG antibody. Furthermore, the protein band intensity was comparable to that of the pEGFP control vector,

indicating successful transcription and translation. This preliminary expression check validated the functionality of the pVP40-FLAG construct and justified its use in the subsequent large-scale production of lentiviral particles.

3. Production and Titration of Pseudotyped Lentiviral Particles

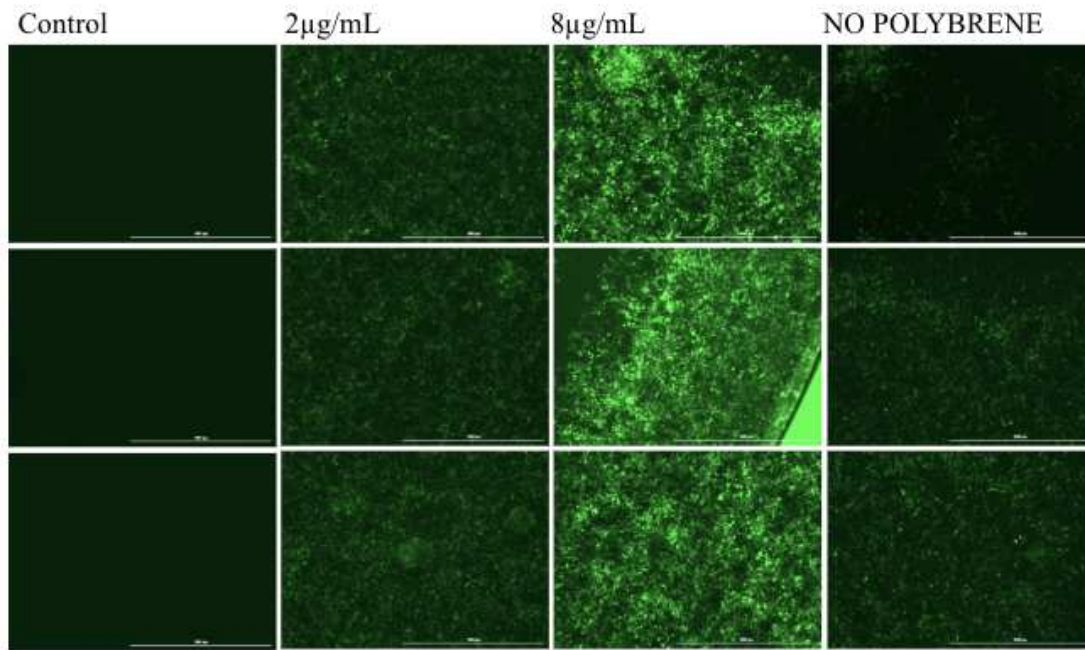
HEK293T producer cells were transfected with the VP40-FLAG or GFP lentiviral vectors together with packaging plasmids. Transfection efficiencies were reproducibly high, as indicated by strong GFP fluorescence in the GFP-transfected control wells. Viral supernatants were collected at 48 h post-transfection. Functional titration on HEK293T cells yielded a mean titer of approximately 2×10^6 TU mL⁻¹ across preparations, which was sufficient for downstream transduction assays.

4. Optimization of Lentiviral Production and Target Cell Transduction

To establish a robust production pipeline, lentiviral vectors were generated in HEK293T cells using two transfection methods. Initial trials with calcium phosphate precipitation resulted in variable transfection efficiency and increased cytotoxicity. Subsequently, the TransIT-LT1 reagent was adopted for all production runs, which consistently yielded higher viral titers and improved cell viability during the production phase. For transduction of the target Huh-7 cell line, parameters known to enhance lentiviral entry were systematically tested.

The inclusion of polybrene at a concentration of 2 µg/mL, combined with spinoculation (2300 × g, 1 h, 20°C), was found to be necessary to achieve detectable transgene expression. This optimized protocol was used as the baseline for all subsequent transduction experiments comparing Huh-7 and HEK293T cells.

HEK293T



Huh-7

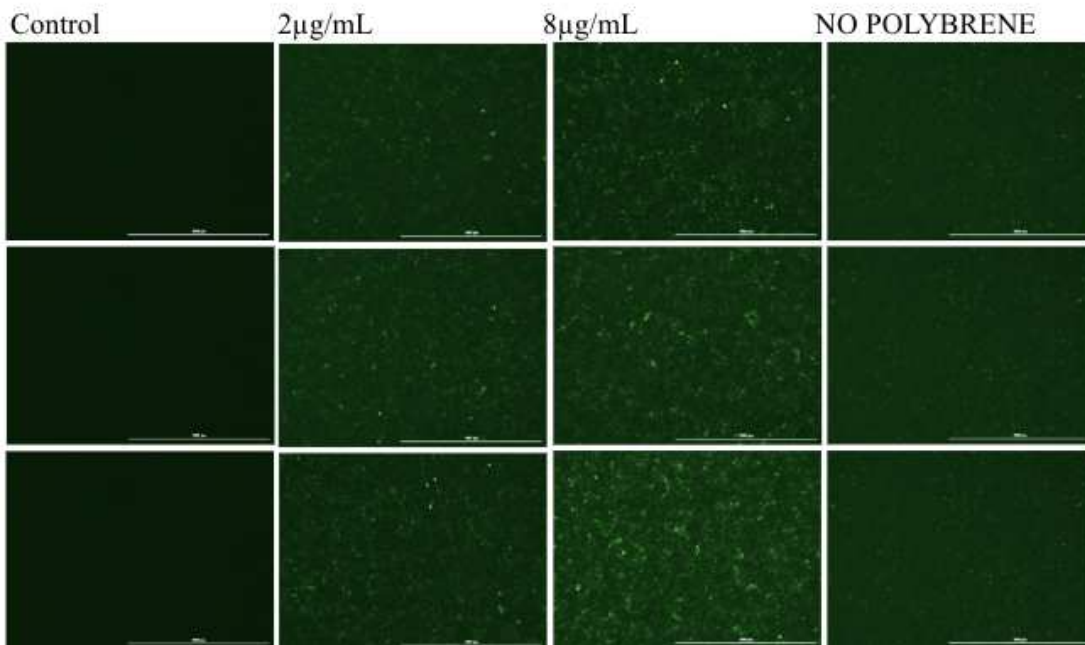


Figure 3. Effect of Polybrene Concentration on Transduction Efficiency. Representative widefield fluorescence microscopy images of HEK293T (A) and Huh-7 (B) cells transduced with GFP-lentivirus (MOI 0.5) under varying concentrations of polybrene. (A) HEK293T cells exhibit high permissiveness with widespread GFP expression even in the absence of polycation, reaching saturation at 5 μ g/mL. (B) Huh-7 cells show a marked dependency on polybrene for entry. In the absence of polybrene, transduction is negligible. Addition of polybrene ($\geq 2 \mu$ g/mL)

significantly increases the proportion of GFP-positive cells, visually confirming the necessity of chemical adjuvants for this restrictive cell line. Images were acquired with constant exposure settings to allow qualitative comparison. Scale bar = 1000 μm .

5. Cell Viability Following Lentiviral Transduction

5.1 HEK293T Cells

Untransduced HEK293T controls displayed consistently high viability (97.6 – 98.4%, $n = 3$). Cells transduced at MOI 0.5 exhibited a modest reduction in viability (mean $71.0 \pm 1.9\%$, $n = 3$). A low-MOI condition produced higher viability (85.4%), whereas a high-MOI condition (MOI 1) resulted in further reduction (57.9%). Mock-transduced samples and handling controls (>97%) showed that viability decreases were associated with exposure to viral particles.

5.2 Huh-7 Cells

Untransduced Huh-7 controls also maintained high viability (97.0–97.8%, $n = 3$). Under baseline transduction conditions (MOI 0.5), viability decreased substantially (mean $29.4 \pm 1.0\%$, $n = 3$). An additional replicate set yielded values of $34.3 \pm 1.1\%$. Low-MOI transduction improved viability (45.2%), whereas high-MOI transduction reduced it further (20.0%). Mock and enhancer-only controls remained above 97%.

Cell viability under different lentiviral transduction conditions

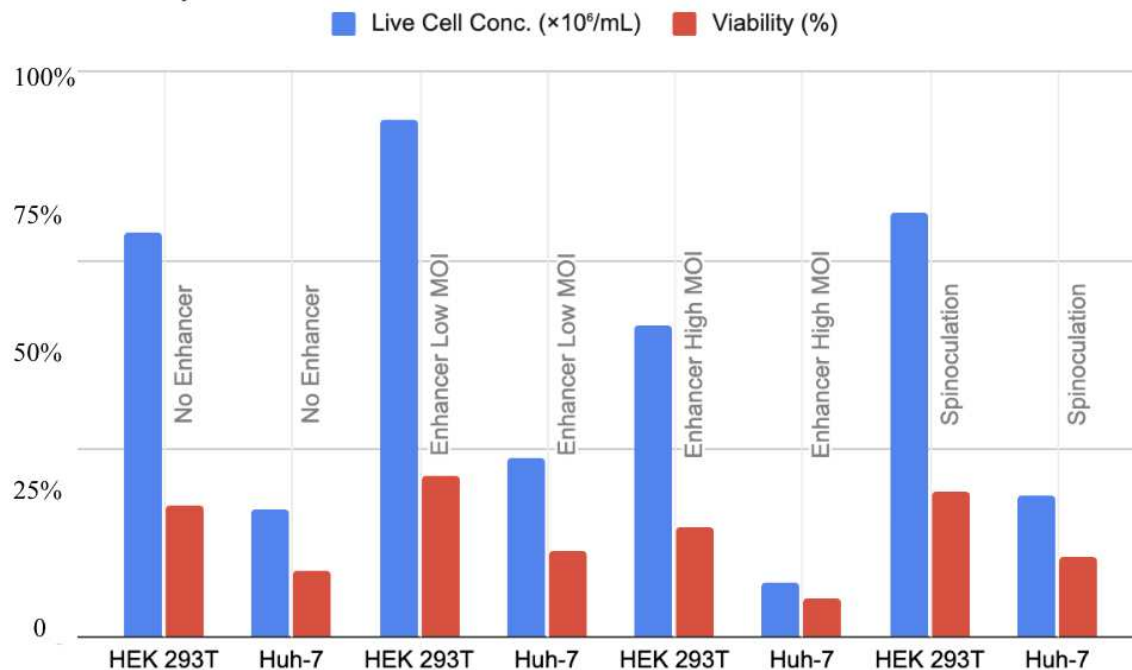


Figure 4. Impact of Transduction Optimization Strategies on Cell Density and Viability in HEK293T and Huh-7 Cell Lines. Quantitative assessment of transduction-associated cytotoxicity assessed at 48 hours post-infection. Raw values for live cell concentration ($\times 10^6$ cells/mL) and

percentage viability determined by Trypan Blue exclusion. Dual-metric analysis comparing HEK293T and Huh-7 cells across four conditions: passive transduction ("No Enhancer"), Polybrene-mediated entry ("Enhancer") at Low and High MOI, and Spinoculation. Blue Bars: Live Cell Concentration ($\times 10^6$ cells/mL). Red Bars: Viability (displayed as a decimal fraction of total population, where 1.0 = 100%). Interpretation: While HEK293T cells maintain robust growth and high viability (>50%) under all conditions, Huh-7 cells exhibit significant susceptibility to transduction stress. Notably, the "High MOI + Enhancer" condition induces severe cytotoxicity in Huh-7 cells (viability drop to 20%; cell density collapse to 0.29×10^6 cells/mL), highlighting the critical physiological trade-off required to achieve viral entry in this restrictive hepatic model.

6. Expression of GFP and VP40-FLAG Assessed by Western Blotting

6.1 Comparison Between HEK293T and Huh-7 Cells

Western blotting detected both GFP and VP40-FLAG in lysates from HEK293T and Huh-7 cells. GAPDH was used as a loading control. Densitometric quantification ($n = 3$, normalized to GAPDH) showed that HEK293T cells expressed VP40-FLAG at 3.85 ± 0.32 arbitrary units and GFP at 3.20 ± 0.25 . In Huh-7 cells, normalized VP40-FLAG and GFP intensities were 0.95 ± 0.15 and 0.80 ± 0.10 , respectively.

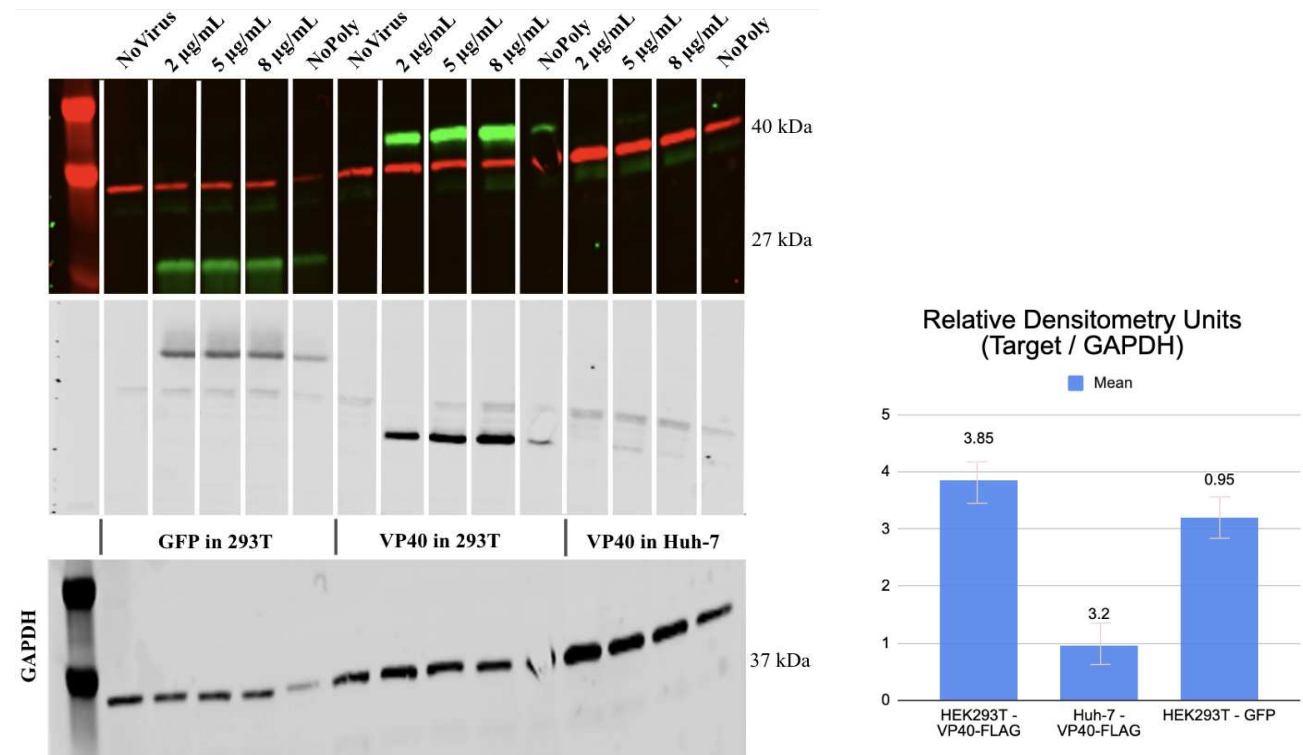


Figure 5. Comparative Analysis of Transgene Expression in HEK293T vs. Huh-7 Cells. (Left) Representative Western blots evaluating the effect of polybrene concentration (0 - 8µg/mL) on

transduction efficiency. Membranes were probed for VP40-FLAG (Green, ~40 kDa) or GFP (Green, ~27 kDa) and normalized to the GAPDH loading control (Red, ~37 kDa). Note the complete absence of signal in the "No Polybrene" lanes for Huh-7 cells, confirming the strict requirement for cationic enhancement in this restrictive line. (Right) Densitometric quantification (mean \pm SD, n=3) of the optimized condition (8 μ g/mL Polybrene). HEK293T cells exhibited significantly higher normalized protein levels (VP40-FLAG: 3.85 ± 0.32) compared to Huh-7 cells (VP40-FLAG: 0.95 ± 0.15), representing a ~4-fold reduction in expression efficiency in the hepatocyte model ($p < 0.01$, Student's t-test).

6.2 MOI-Dependent VP40-FLAG Expression in Huh-7 Cells

To evaluate dose-response, Huh-7 cells were transduced at MOI 0.25, 0.5, and 1. VP40-FLAG was detected under all conditions. Densitometry indicates an MOI-dependent increase in normalized VP40-FLAG intensity: 0.80 ± 0.10 (MOI 0.25), 1.90 ± 0.20 (MOI 0.5), and 2.80 ± 0.35 (MOI 1). GAPDH levels remained uniform across samples.

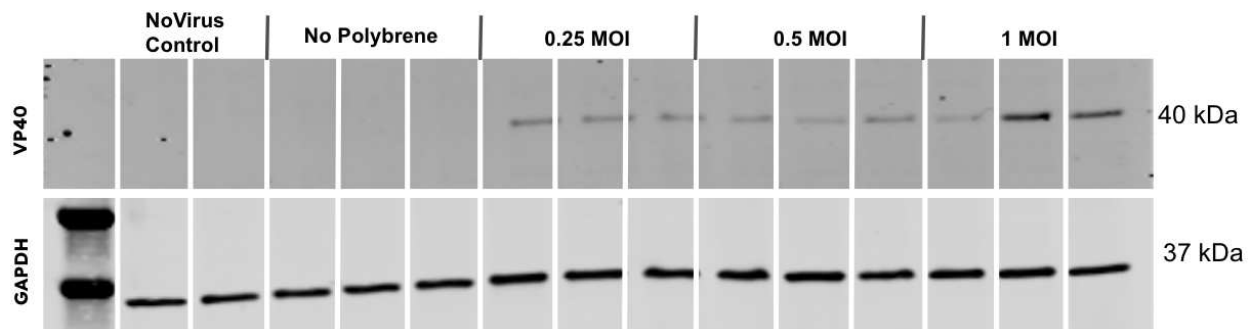


Figure 6. MOI-dependent VP40-FLAG expression in Huh-7 cells.

Western blot analysis of Huh-7 cells transduced with VP40-FLAG lentivirus at MOIs of 0.25, 0.5, and 1. GAPDH is shown as loading control. Densitometric quantification (n=3, mean \pm SD) normalized to GAPDH indicates a dose-dependent increase in VP40-FLAG protein levels (MOI 0.25: 0.80 ± 0.10 ; MOI 0.5: 1.90 ± 0.20 ; MOI 1: 2.80 ± 0.35), validating the quantitative control offered by the lentiviral system.

7. Generation of Stably Transduced Huh-7 Cells

Stable Huh-7 cell populations expressing GFP or VP40-FLAG were generated by antibiotic selection following lentiviral transduction. A blasticidin kill-curve performed in preliminary optimization experiments established that concentrations between 5 and 10 μ g/mL effectively eliminated non-transduced cells within 7–10 days. Based on this assessment, a working concentration of 6 μ g/mL was applied to derive homogeneous resistant populations. Surviving cells expanded uniformly and maintained stable fluorescence or VP40-FLAG expression

throughout subsequent passaging, confirming successful generation of stably transduced lines suitable for downstream characterization.

8. Qualitative Assessment of Transduction Efficiency by Confocal Microscopy

Confocal microscopy was performed to visualize transduction outcomes using GFP-encoding lentiviral particles. HEK293T cells displayed numerous GFP-positive cells with high fluorescence intensity. Huh-7 cells exhibited fewer positive cells with lower overall signal intensity.

Manual counts of GFP-positive (P) and DAPI-stained nuclei (N) were used to estimate transduction efficiency. HEK293T cells showed a mean efficiency of $24 \pm 4.5\%$, whereas Huh-7 dense fields yielded $12 \pm 3.0\%$. These values correspond to the visual differences observed in the micrographs.

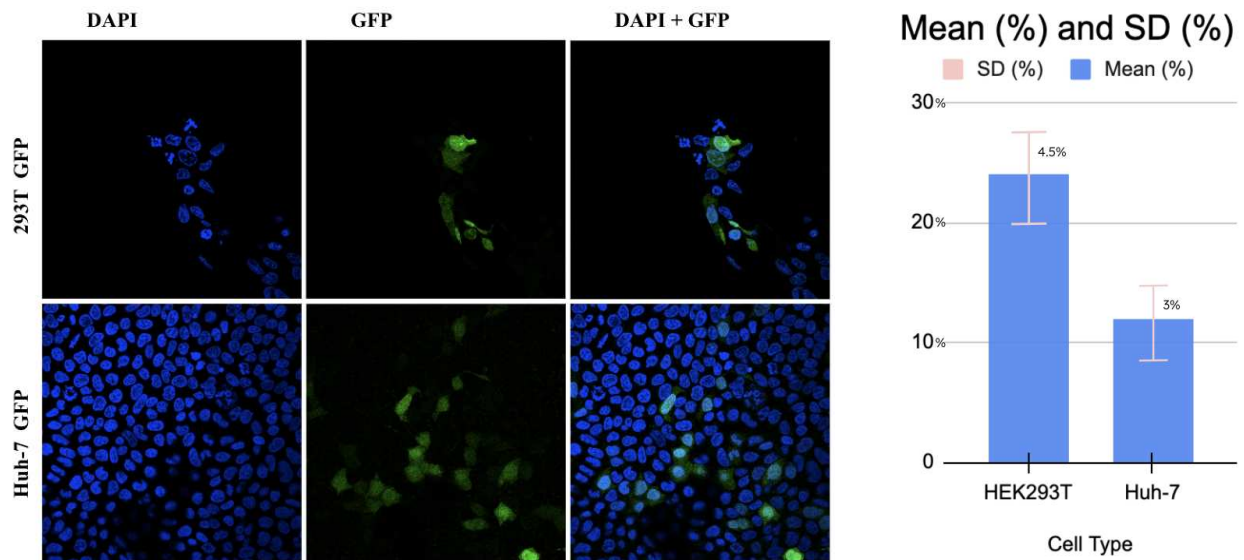


Figure 7. Confocal microscopy of GFP-expressing HEK293T and Huh-7 cells.

Representative confocal images showing GFP fluorescence (green) and DAPI-stained nuclei (blue). Scale bar: 40 μm . Corresponding transduction efficiency values were calculated by manual quantification of GFP-positive and DAPI-positive cells.

IV. DISCUSSION

1. Overall Significance and the Necessity of Physiologically Relevant BSL-2 Platforms

VP40 as the Linchpin of Assembly and a Therapeutic Target

The Ebola virus matrix protein (VP40) is the master regulator of viral morphogenesis. It is the minimal determinant required for the budding of filamentous virions, a process driven by its ability to oligomerize into hexameric lattices at the plasma membrane and recruit host ESCRT machinery [3, 21]. Given its pivotal role in the viral life cycle and its high sequence conservation across Ebolavirus species, VP40 represents a critical target for broad-spectrum antiviral intervention [6]. However, the study of VP40 biology has been historically bifurcated: high-containment (BSL-4) laboratories utilize authentic virus but suffer from low throughput, while accessible BSL-2 laboratories rely heavily on plasmid-based VLP systems that generate non-physiological protein levels [8, 44].

This study bridges this methodological gap by validating a third-generation lentiviral delivery system for VP40. By moving away from transient overexpression, this platform provides a stable, biosafety-compliant tool to dissect the molecular mechanics of assembly—such as lipid binding and membrane curvature [3, 13]—under conditions that more closely approximate the stoichiometric constraints of a natural infection.

Relevance to Vaccine and Antiviral Development

The significance of this platform extends beyond basic virology. VP40 is a key component of current vaccine strategies; for instance, Virus-Like Particles (VLPs) generated by VP40 expression are potent immunogens that can elicit protective neutralizing antibodies when co-expressed with the Glycoprotein (GP) [27, 28]. However, the efficiency of VLP production is a major bottleneck for manufacturing. Current industrial methods often rely on transient transfection of HEK293T cells, which is difficult to scale and costly [44]. The lentiviral approach established here demonstrates the feasibility of generating stable, constitutive producer lines, a strategy that could be adapted for large-scale VLP vaccine production, similar to methods used for other enveloped viruses [37].

Furthermore, the tunable nature of lentiviral expression makes this system ideal for cell-based antiviral screening. Recent high-throughput campaigns have identified small molecules capable of disrupting VP40 oligomerization [6, 24]. Validating these hits requires a cellular model where VP40 levels are controlled; grossly overexpressed protein can artificially shift the IC-50 values of candidate drugs, leading to false negatives [6]. By enabling precise titration of VP40 via MOI modulation, this Huh-7 model offers a more rigorous platform for the pre-clinical evaluation of next-generation filovirus therapeutics [32].

Modeling the Hepatic Context of Infection

Finally, the successful transduction of Huh-7 cells addresses a critical gap in modeling the host-pathogen interface. While HEK293T cells are the standard "protein factory" for VLP research [44], they are of kidney origin and lack the metabolic profile of the liver, a primary organ of EBOV replication and pathology [17, 19]. Hepatocytes possess unique lipid metabolic pathways that regulate the levels of Phosphatidylserine (PS) and PI(4,5)P₂, the anionic lipids strictly required for VP40 membrane anchoring [13, 30]. By establishing VP40 expression in a hepatocyte-derived background, this study paves the way for investigating how liver-specific host factors—such as innate immune sensors or lipid kinases—modulate viral assembly and egress, interactions that are likely lost in non-relevant cell lines [22].

2. Optimization of Lentiviral Production and Delivery

Enhancing Vector Quality via Lipid-Based Transfection

The first critical bottleneck in establishing a reliable delivery system is the generation of high-titer viral supernatants. In this study, we compared the traditional Calcium Phosphate (CaPO₄) precipitation method against a lipid-based reagent (TransIT-LT1). While CaPO₄ is widely used due to its low cost, our results indicated significant batch-to-batch variability and higher cytotoxicity in the HEK293T producer cells. This aligns with established literature suggesting that CaPO₄ efficiency is notoriously sensitive to minor fluctuations in pH and buffer composition, which can lead to the formation of large, toxic precipitates that reduce cell viability and viral yield [37, 44]. In contrast, the switch to the lipid-based reagent yielded consistent, high-titer preparations (>10⁶, TU/mL). This consistency is crucial for downstream applications; by ensuring a robust supply of virions, we minimize the confounding variable of "input dose" when comparing transduction efficiencies across different cell lines [37].

Overcoming the Electrostatic Barrier in Hepatocytes

While VSV-G pseudotyping confers broad tropism by targeting the ubiquitous LDL receptor, entry into hepatocyte-derived lines like Huh-7 remains inefficient compared to HEK293T cells [1, 41]. This study confirmed that "passive" transduction is insufficient for these restrictive cells. The addition of Polybrene (hexadimethrine bromide) was identified as a critical factor for success. Mechanistically, Polybrene is a cationic polymer that neutralizes the electrostatic repulsion between the negatively charged viral envelope and the sialic acid residues on the plasma membrane, facilitating adsorption [38].

However, our optimization data highlighted a delicate therapeutic window: while polybrene $\geq 2\mu\text{g/mL}$ were necessary for entry, concentrations exceeding $8\mu\text{g/mL}$ triggered significant cytotoxicity in Huh-7 cells. This "double-edged sword" effect of polycations is well-documented

in difficult-to-transduce targets, such as mesenchymal stem cells and primary hepatocytes [38, 41].

The Role of Spinoculation

Finally, we demonstrated that chemical adjuvants alone were insufficient to maximize gene transfer. The application of spinoculation (2300 x g centrifugation) significantly enhanced transduction efficiency. This process works by overcoming the diffusion limits of viral particles (Brownian motion), mechanically sedimenting virions onto the cell surface to increase the multiplicity of infection at the plasma membrane interface [38]. By combining envelope pseudotyping (VSV-G), charge neutralization (Polybrene), and mechanical sedimentation (Spinoculation), this optimized protocol overcomes the intrinsic resistance of the Huh-7 model, establishing a reproducible pipeline for VP40 expression that would not be achievable with standard protocols [36].

3. Balancing Reductionism and Biological Relevance

The Strategic Choice of a Reductionist Model

The conceptual framework of this study was deliberate: to establish a platform for delivery fidelity, rather than to simulate the chaotic environment of a full viral infection. While authentic infection involves a complex interplay of seven viral proteins, VP40 alone is the minimal determinant for matrix assembly and VLP egress [20]. By isolating VP40 from the nucleocapsid (NP) and glycoprotein (GP), this study adopts a reductionist approach that allows for the dissection of matrix-specific functions—such as membrane curvature induction and ESCRT recruitment—without the confounding variables of viral replication or GP-mediated cytotoxicity [3, 11]. This isolation is critical for validating potential inhibitors that target the matrix assembly step specifically, ensuring that observed effects are due to direct target engagement rather than off-target interference with viral entry or transcription [6].

The Rationale for Low MOI and Single-Copy Integration

A key finding of this study was the modulation of transduction efficiency in HEK293T cells, which settled at a mode of $24\% \pm 4.5\%$ under baseline conditions (MOI 0.5). It is crucial to interpret this value not as a limitation of viral titer, but as a direct consequence of the experimental design aimed at achieving single-copy integration. According to the Poisson distribution governing viral entry, targeting a transduction efficiency of $\sim 20\text{-}30\%$ ensures that the vast majority of transduced cells harbor a single proviral integration event [37].

In contrast, aiming for maximal transduction (100%) typically requires high MOIs ($> 5 - 10$), which leads to multiple integration events per genome. Multiple integrations create a heterogeneous cell population where protein expression variance is driven by copy number rather than biological regulation [35, 42]. By deliberately restricting the MOI to 0.5, this platform

prioritizes the generation of a homogeneous population with defined genetic content. This standardization is essential for future mechanistic studies, as it minimizes the risk of insertional mutagenesis or promoter interference affecting the cellular phenotype [35, 42].

Unlocking the Study of Concentration-Dependent Oligomerization

The ability to titrate VP40 expression is the defining advantage of this lentiviral system over plasmid-based alternatives. VP40 is a pleomorphic protein whose function is strictly dictated by its oligomeric state, which in turn is concentration-dependent [9]. At low concentrations early in the lifecycle, VP40 forms octameric rings that bind RNA and regulate transcription; as concentration rises, it transitions into membrane-associated hexamers that drive budding [5, 16].

Transient transfection creates an immediate "burst" of protein that likely forces the equilibrium toward the hexameric state, bypassing the early regulatory forms. The linear scaling of VP40 expression observed in this study confirms that the lentiviral platform allows for the precise "dialing up" of intracellular protein concentration [37]. This capability provides a unique opportunity to study the molecular triggers of the octamer-to-hexamer switch in a controlled cellular environment, a level of mechanistic resolution that is inaccessible in overexpression models [21].

4. Cell-Type Dependence and Functional Consequences

Mechanisms of Permissiveness: HEK293T vs. Huh-7

The marked dichotomy in transduction efficiency observed between HEK293T and Huh-7 cells highlights the critical influence of the host cellular environment on lentiviral vector biology. HEK293T cells exhibited high transgene expression even in the absence of chemical adjuvants, a result consistent with their status as the "gold standard" for vector production. These cells are transformed with the SV40 large T-antigen and are functionally deficient in several innate immune sensing pathways, rendering them highly permissive to foreign nucleic acid entry and expression [44].

In contrast, the restrictive nature of Huh-7 cells, which required both polycationic neutralization (Polybrene) and mechanical sedimentation (spinoculation) to achieve detectable VP40 levels, reflects their retained hepatocyte identity. Hepatocytes possess robust innate defense mechanisms, including functional RIG-I and TLR3 signaling pathways, which can detect lentiviral RNA reverse transcription intermediates and trigger an antiviral state that suppresses transgene expression [30]. Furthermore, while VSV-G pseudotyping targets the Low-Density Lipoprotein Receptor (LDLR)—which is present on hepatocytes—the surface density and recycling kinetics of these receptors in Huh-7 cells may differ from the optimized display on HEK293T cells, creating a rate-limiting step for viral entry [1, 36]. The finding that VP40 expression scales linearly with MOI in this restrictive background is therefore a significant

validation; it proves that once the entry barrier is overcome, the intracellular machinery for CMV-driven transcription remains functional and dose-responsive [37].

The "Double-Edged Sword" of Transduction Enhancement

A critical limitation identified in this study was the substantial cytotoxicity associated with the conditions necessary to overcome Huh-7 resistance. The observation that cell viability plummeted to ~30% under high-load conditions (MOI > 1.0, Polybrene 8µg/mL) aligns with the "double-edged sword" of physicochemical transduction enhancement described in the literature [38].

This toxicity is likely multifactorial. First, Polybrene acts by destabilizing the plasma membrane to facilitate viral fusion; at high concentrations, this destabilization compromises membrane integrity, leading to necrotic cell death [38]. Second, the VSV-G envelope itself is known to be cytotoxic when accumulated at high multiplicities; its fusogenic activity can induce syncytia formation and disrupt cellular homeostasis [42]. This data strongly suggests that the observed lethality is not an artifact of the VP40 protein itself, but a consequence of the vector delivery vehicle interacting with a sensitive host membrane [41].

Metabolic Implications for VLP Assembly

The functional consequence of this transduction-associated stress is the most profound implication of this study. VP40-driven egress is not a passive event; it is an energy-intensive process that relies on the host's metabolic health. Specifically, the recruitment of the ESCRT machinery (particularly the ATPase Vps4) to facilitate the final membrane scission of the budding virion requires a robust supply of cellular ATP [21].

In cells exhibiting ~70% mortality (as seen in the high-MOI Huh-7 condition), metabolic depletion and the activation of stress pathways such as the Unfolded Protein Response (UPR) are likely to stall the budding machinery [5]. Furthermore, the membrane damage induced by polybrene may disrupt the precise lipid microdomains (PI(4,5)P₂ patches) required for VP40 oligomerization [13]. Therefore, the "low budding" efficiency often reported in restrictive cells may be partially attributable to vector-induced metabolic collapse rather than intrinsic viral restriction. This finding emphasizes that future BSL-2 screens must prioritize the "therapeutic window" of transduction—balancing expression level against metabolic viability—to avoid confounding viral restriction with cellular morbidity [5, 17].

5. Confocal Microscopy as Qualitative Validation of Delivery Fidelity

Visualizing the "Permissiveness Gap"

Confocal imaging provided a crucial, spatially resolved complement to the bulk population data obtained via Western blotting. While immunoblotting quantifies total protein accumulation, it

cannot distinguish between a scenario of uniform low expression versus high expression in a small subpopulation. The confocal analysis resolved this ambiguity: HEK293T cells displayed a uniform, high-intensity GFP signal indicative of high multiplicity of infection (MOI) and unhindered promoter activity [2, 44].

In stark contrast, the Huh-7 population revealed a significant degree of heterogeneity. Even under optimized conditions (Polybrene/Spinoculation), the GFP signal was mosaic, with some cells displaying robust expression while adjacent cells remained negative. This "mosaicism" likely reflects the stochastic nature of lentiviral entry into restrictive cells, where the probability of overcoming the innate immune barrier or engaging a limiting receptor (LDLR) varies cell-to-cell [36]. Furthermore, this heterogeneity may indicate silencing of the CMV promoter in specific sub-lineages of the hepatocyte population, a known limitation of using viral promoters in differentiated tissue models [40].

Methodological Advantages of Native Fluorescence

A key strength of this validation step was the reliance on native GFP fluorescence rather than immunofluorescence (IF). IF protocols require fixation (paraformaldehyde) and permeabilization (detergents like Triton X-100) to allow antibody access. These processing steps can artificially extract membrane lipids and alter cellular morphology, potentially confounding the assessment of viral vector performance [1]. By utilizing the intrinsic fluorescence of the reporter, we established a "live-cell compatible" baseline for transduction efficiency that is free from antibody-binding artifacts or epitope masking, serving as a direct and unambiguous readout of the vector's functional entry and integration [37].

Future Directions: Defining the Subcellular Localization of VP40

While the current study utilized GFP to validate the delivery pipeline, the ultimate utility of this platform lies in resolving the subcellular distribution of VP40 itself. Future studies must employ anti-FLAG immunostaining to confirm that the lentivirally expressed VP40 is biologically active. Specifically, microscopy should distinguish between two distinct phenotypes described in the literature:

1. The Transport Phenotype: Perinuclear accumulation, indicative of VP40 engaging the COPII transport machinery (Sec24C) for trafficking to the plasma membrane [7, 22].
2. The Assembly Phenotype: Enrichment at the plasma membrane inner leaflet, specifically in phosphatidylserine (PS) and PI(4,5)P₂-rich microdomains [13].

The observation of filamentous projections extending from the cell surface would provide the definitive morphological proof that the lentiviral system produces VP40 at the correct stoichiometric threshold to trigger the "conformational switch" from dimers to hexameric lattices [5, 21]. Conversely, a diffuse cytoplasmic signal would suggest that the Huh-7

cellular environment (e.g., lipid composition or restriction factors) is suppressing assembly, a mechanistic insight that only this imaging-based platform can provide [8].

6. Limitations of This Study

The Gap Between Expression and Functional Assembly

The primary limitation of this work lies in the distinction between protein accumulation and functional assembly. While Western blotting and confocal microscopy successfully confirmed the expression of full-length VP40-FLAG, these assays do not definitively prove that the protein has successfully oligomerized into the hexameric lattices required for egress [15, 21]. In overexpression systems, VP40 can occasionally form intracellular aggregates or be degraded via the proteasome without ever being released as a virus-like particle (VLP) [1]. Consequently, the current dataset cannot distinguish between "competent assembly" and "abortive trafficking." Future validation will require physical separation techniques, such as sucrose gradient ultracentrifugation or Nanoparticle Tracking Analysis (NTA), to isolate and quantify budding VLPs from the culture supernatant, thereby providing the definitive functional readout of the system's biological fidelity [20, 25].

Resolution Limits of Bulk Analysis

Secondly, the reliance on bulk-population assays (immunoblotting) obscures the single-cell dynamics of the restrictive Huh-7 model. While densitometry provided an average measure of expression, the heterogeneity observed in the confocal data suggests a complex landscape of transduction where some cells are highly permissive while neighbors remain refractory [36]. The lack of Flow Cytometry (FACS) analysis prevents the precise quantification of this "transduction mosaicism." Without single-cell resolution, it is impossible to determine whether the lower expression in Huh-7 cells results from a uniform reduction in promoter activity (transcriptional silencing) or a stochastic "all-or-nothing" entry barrier [35, 40]. This distinction is critical for downstream screening applications, where population heterogeneity can introduce significant noise into inhibitor potency (IC-50) calculations [6].

The Confounding Variable of Cytotoxicity

Thirdly, the substantial cytotoxicity observed under high-load transduction conditions (MOI > 1.0, Polybrene > 8 μ g/mL) introduces a major confounding variable. Cellular stress is not merely a side effect; it is a direct disruptor of the viral life cycle. EBOV budding is intimately linked to host cell homeostasis; specifically, the induction of apoptosis (via Caspases) or the activation of the Unfolded Protein Response (UPR) can independently cleave viral proteins or arrest the secretory pathway [17, 43]. In cells exhibiting ~30% viability, the bioenergetic depletion of ATP may stall the ATPase Vps4, which is required to recycle the ESCRT complexes during membrane scission [21]. Therefore, any reduction in VLP output observed under these harsh

conditions could be misattributed to viral restriction when it is, in fact, a consequence of metabolic collapse.

Promoter Constraints and Temporal Artificiality

Finally, while the use of a constitutive CMV promoter was necessary for this proof-of-concept study, it does not recapitulate the temporal logic of an authentic infection. During natural EBOV replication, VP40 accumulation is delayed relative to the nucleocapsid (NP) to prevent premature encapsidation [16]. Constitutive expression bypasses this "timer," potentially forcing interactions between VP40 and host factors that would normally be segregated temporally. This artificial kinetics limits the system's ability to model the very early events of matrix assembly, where low protein concentrations favor the transcriptional-regulatory octamer state over the budding-competent hexamer [3, 5]. Future iterations of this platform should explore inducible promoters (e.g., Tet-On systems) to restore this temporal dimension and better mimic the progressive accumulation of viral antigens [40].

V. CONCLUSIONS

1. Synthesis of Findings and Validation of the Platform

In conclusion, this thesis has successfully engineered and validated a quantitative lentiviral delivery system for the Ebola virus matrix protein VP40, effectively bridging the methodological gap between artifact-prone plasmid overexpression and high-containment infection models [1, 8]. By constructing a biosafety-compliant third-generation transfer vector and systematically optimizing the transduction protocol—specifically identifying the critical requirement for cationic neutralization (Polybrene) and mechanical enhancement (spinoculation)—this study overcame the intrinsic entry barriers of the restrictive Huh-7 hepatocyte line [1, 41]. The experimental evidence confirms that this optimized pipeline enables the reproducible expression of VP40 in a biologically relevant human liver background, fulfilling the primary objective of establishing a safer, scalable BSL-2 scaffold for filovirus research.

2. Quantitative Fidelity and Stoichiometric Control

The densitometric and microscopic analyses provided definitive proof of the system's controllability. While quantitative comparison revealed a statistically significant, approximate four-fold reduction in VP40 accumulation in Huh-7 cells relative to the permissive HEK293T benchmark, this "restriction" serves as a biological validation of the model's physiological fidelity. It confirms that the Huh-7 system retains the innate defense mechanisms characteristic of natural target tissue, unlike the deregulated environment of transformed kidney cells [19, 30]. Crucially, the study demonstrated a linear, dose-dependent scaling of VP40 protein levels in response to increasing Multiplicity of Infection (MOI). This predictable tunability is the defining advantage of the platform. Unlike the "all-or-nothing" expression profile of transient

transfection, this linear dynamic range provides the necessary resolution to investigate concentration-dependent molecular events, such as the critical switch between VP40's transcriptional-regulatory oligomers and its assembly-competent hexameric lattices [5, 15].

3. Highlighting Achievements and Reconciling Limitations

The principal value of this work lies in the prioritization of delivery fidelity over raw protein yield. By deliberately establishing a low-MOI baseline (0.5), the system was engineered to favor single-copy genomic integration events [35, 42]. This strategy minimizes the stochastic noise associated with multi-copy concatemers and prevents the formation of supraphysiological protein aggregates often seen in plasmid-based systems [1, 37]. Consequently, this platform provides a homogeneous cellular environment where VP40 expression is driven by defined genetic elements rather than transfection efficiency artifacts. This "clean" background is a prerequisite for future mechanistic studies aiming to deconstruct the subtle electrostatic requirements for matrix assembly without the confounding variables of cellular stress or promoter saturation [3, 5]. Ultimately, this optimized platform successfully bridges the operational gap between oversimplified, artifact-prone plasmid models and the logistical bottleneck of high-containment infection studies [1, 8].

4. The Bioenergetic Cost of Transduction

However, the optimization process revealed a critical biological trade-off. The physicochemical conditions required to overcome the entry barriers of Huh-7 cells (Polybrene $>5\mu\text{g/mL}$ and VSV-G load) imposed a substantial cytotoxic burden, reducing viability to $\approx 30\%$ at the upper limits of the tested range [38, 41]. This severe cellular stress represents the defining boundary condition of the model. VLP budding is not a passive biophysical event; it is an energy-intensive process that relies on the host's metabolic health to power the ESCRT machinery, particularly the ATP-dependent disassembly of ESCRT-III filaments by Vps4 [21]. In metabolically compromised cells, the depletion of intracellular ATP pools could stall the scission machinery, leading to an "abortive budding" phenotype that mimics viral restriction [17]. Therefore, while the system provides unprecedented genetic control, the "therapeutic window" for transduction must be strictly enforced to ensure that downstream functional assays reflect authentic viral biology rather than vector-induced metabolic collapse.

5. Future Directions

An immediate priority for the evolution of this platform is the refinement of the expression kinetics. The current reliance on the constitutive CMV promoter, while effective for proof-of-concept, drives rapid protein accumulation that can overwhelm cellular trafficking pathways and induce metabolic stress [17]. Future iterations should incorporate inducible expression systems (e.g., Tetracycline-On or Ecdysone-responsive elements) to allow for the precise temporal initiation of VP40 synthesis [40]. This would enable researchers to trigger

expression only after the cell population has recovered from transduction-associated stress, thereby separating vector toxicity from viral biology. Furthermore, exploring hepatocyte-specific promoters (e.g., Albumin or α -1 antitrypsin) could restrict expression to differentiated cells, reducing off-target effects in mixed culture models and enhancing the physiological relevance of the hepatic system [41].

Moving from Expression to Functional Quantification

Following vector optimization, the analytical focus must shift from intracellular accumulation to extracellular release. To definitively validate the budding competency of the lentivirally expressed VP40, rigorous quantitative assays must be implemented. Nanoparticle Tracking Analysis (NTA) and Sucrose Gradient Ultracentrifugation will be essential to physically separate and quantify bona fide Virus-Like Particles (VLPs) from cellular debris or exosomes [20, 25]. Establishing a robust correlation between intracellular VP40 levels (MOI) and VLP output is the critical missing link required to mathematically model the "tipping point" of assembly—the specific concentration at which dimeric VP40 initiates lattice polymerization [3, 21].

Reconstituting the Viral RNP and Envelope

To advance beyond a simple budding model, the system's biological complexity should be incrementally increased by introducing other structural proteins. Co-transduction with lentiviral vectors encoding the Nucleoprotein (NP) and Glycoprotein (GP) would allow for the study of determining factors in nucleocapsid recruitment and envelope incorporation, processes that are strictly regulated by specific domains on VP40 [18, 19]. This stepwise reconstruction would effectively create a "modular" trVLP system, enabling the controlled investigation of how specific mutations (e.g., in the GP mucin domain) influence entry and assembly in a liver-specific context without the safety risks of a replication-competent virus [1, 11].

Scalable Screening for Host Factors and Antivirals

Finally, the defining potential of this stable, tunable platform lies in its scalability for translational research. Unlike transient transfection, which varies batch-to-batch, a stable lentiviral cell line provides the uniform baseline necessary for CRISPR-Cas9 genetic screens. This could be leveraged to systematically identify essential host dependencies—such as specific lipid kinases or novel ESCRT isoforms—that regulate VP40 egress in hepatocytes [22, 30]. Ultimately, this optimized model serves as an ideal scaffold for medium-throughput phenotypic screening of small-molecule libraries. By quantifying the reduction of VLP release in a biosafety-compliant setting, this platform can accelerate the discovery of novel "assembly inhibitors" that complement existing entry-targeted therapeutics, addressing the urgent need for broad-spectrum intervention strategies against filoviruses [6, 24, 32].

VI. REFERENCES

- Bodmer B.S., Hoenen T., Wendt L. (2024) Molecular Insights into the Ebola Virus Life Cycle. *Nat Microbiol* 9:1417-1426. <https://doi.org/10.1038/s41564-024-01703-z>
- Breen K.M., Haar M.E., Klatt C.L., Halaszynski K.L., Ridenhour C.J., Billbrey A.E., et al. (2024) PI(4,5)P2 Binding Sites in the Ebola Virus Matrix Protein VP40 Modulate Assembly and Budding. *J Lipid Res* 65(3):100512. <https://doi.org/10.1016/j.jlr.2024.100512>
- Broni E., Ashley C., Adams J., Manu H., Aikins E., Okom M., et al. (2023) Cheminformatics-Based Study Identifies Potential Ebola VP40 Inhibitors. *Int J Mol Sci* 24(7):6298. <https://doi.org/10.3390/ijms24076298>
- Dessen A., Volchkov V., Dolnik O., Klenk H.D., Weissenhorn W. (2000) Crystal Structure of the Matrix Protein VP40 from Ebola Virus. *EMBO J* 19(16):4228-4236. <https://doi.org/10.1093/emboj/19.16.4228>
- Falasca L., Agrati C., Petrosillo N., Di Caro A., Capobianchi M.R., Ippolito G., et al. (2015) Molecular Mechanisms of Ebola Virus Pathogenesis: Focus on Cell Death. *Cell Death Differ* 22:1250-1259. <https://doi.org/10.1038/cdd.2015.67>
- Hoenen T., Groseth A., de Kok-Mercado F., Kuhn J.H., Wahl-Jensen V. (2011) Minigenomes, Transcription and Replication Competent Virus-Like Particles and Beyond: Reverse Genetics Systems for Filoviruses and Other Negative Stranded Hemorrhagic Fever Viruses. *Antiviral Res* 91(2):195-208. <https://doi.org/10.1016/j.antiviral.2011.06.003>
- Hoenen T., Shabman R.S., Groseth A., Herwig A., Weber M., Schudt G., et al. (2012) Inclusion Bodies are a Site of Ebolavirus Replication. *J Virol* 86(21):11779-11788. <https://doi.org/10.1128/JVI.01525-12>
- Hoenen T., Watt A., Mora A., Feldmann H. (2014) Modeling The Lifecycle Of Ebola Virus Under Biosafety Level 2 Conditions With Virus-like Particles Containing Tetracistronic Minigenomes. *J Vis Exp* (91):e52381. <https://doi.org/10.3791/52381>
- Jain S., Martynova E., Rizvanov A., Khaiboullina S., Baranwal M. (2021) Structural and Functional Aspects of Ebola Virus Proteins. *Pathogens* 10:1330. <https://doi.org/10.3390/pathogens10101330>
- Kühl A., Banning C., Marzi A., Votteler J., Steffen I., Bertram S., et al. (2014) The VP40 Protein of Marburg Virus Exhibits Impaired Budding and Increased Sensitivity to Human Tetherin Following Mouse Adaptation. *J Virol* 88(23):13740-13752. <https://doi.org/10.1128/JVI.02069-14>
- Lee J.E., Saphire E.O. (2009) Ebolavirus Glycoprotein Structure and Mechanism of Entry. *Future Virol* 4(6):621-635. <https://doi.org/10.2217/fvl.09.56>

- Messaoudi I., Amarasinghe G.K., Basler C.F. (2015) Filovirus Pathogenesis and Immune Evasion: Insights from Ebola Virus and Marburg Virus. *Nat Rev Microbiol* 13(11):663-676. <https://doi.org/10.1038/nrmicro3524>
- Motsa B.B., Sharma T., Cioffi M.D., Chapagain P.P., Stahelin R.V. (2024) Minor Electrostatic Changes Robustly Increase VP40 Membrane Binding, Assembly, and Budding of Ebola Virus Matrix Protein Derived Virus-Like Particles. *J Biol Chem* 300(5):107213. <https://doi.org/10.1016/j.jbc.2024.107213>
- Mühlberger E., Weik M., Volchkov V.E., Klenk H.D., Becker S. (1999) Comparison of the Transcription and Replication Strategies of Marburg Virus and Ebola Virus by Using Artificial Replication Systems. *J Virol* 73(3):2333-2342. <https://doi.org/10.1128/JVI.73.3.2333-2342.1999>
- Pleet M.L., Mathiesen A., DeMarino C., Akpamagbo Y.A., Barclay R.A., Schwab A., et al. (2017) The Role of Exosomal VP40 in Ebola Virus Disease. *DNA Cell Biol* 36(4):243-250. <https://doi.org/10.1089/dna.2017.3639>
- Reynolds P., Marzi A. (2017) Ebola and Marburg Virus Vaccines. *Virus Genes* 53(4):501-515. <https://doi.org/10.1007/s11262-017-1455-x>
- Rivera A., Messaoudi I. (2016) Molecular Mechanisms of Ebola Pathogenesis. *J Leukoc Biol* 100(5):889-904. <https://doi.org/10.1189/jlb.4RI0316-099RR>
- Spiegelberg L., Wahl-Jensen V., Kolesnikova L., Feldmann H., Becker S., Hoenen T. (2011) Genus-specific Recruitment of Filovirus Ribonucleoprotein Complexes into Budding Particles. *J Gen Virol* 92(Pt 12):2900-2905. <https://doi.org/10.1099/vir.0.036863-0>
- Wan W., Kolesnikova L., Clarke M., Koehler A., Noda T., Becker S., et al. (2017) Structure and Assembly of the Ebola Virus Nucleocapsid. *Nature* 551:394-397. <https://doi.org/10.1038/nature24490>
- Watanabe S., Watanabe T., Noda T., Takada A., Feldmann H., Jasenosky L.D., Kawaoka Y. (2004) Production of Novel Ebola Virus-like Particles from cDNAs: An Alternative to Ebola Virus Generation by Reverse Genetics. *J Virol* 78(2):999-1005. <https://doi.org/10.1128/jvi.78.2.999-1005.2004>
- Winter S.L., Golani G., Lolicato F., Vallbracht M., Thiyagarajah K., Sid Ahmed S., et al. (2023) The Ebola Virus VP40 Matrix Layer Undergoes Endosomal Disassembly Essential for Membrane Fusion. *EMBO J* 42:e113578. <https://doi.org/10.15252/emboj.2023113578>
- Yamayoshi S., Noda T., Ebihara H., Goto H., Morikawa Y., Lukashevich I.S., et al. (2008) Ebola Virus Matrix Protein VP40 Uses the COPII Transport System for Its Intracellular Transport. *Cell Host Microbe* 3(3):168-177. <https://doi.org/10.1016/j.chom.2008.02.001>

- ElSherif M.S., Brown C., MacKinnon-Cameron D., Li L., Racine T., Alimonti J., et al. (2017) Assessing the Safety and Immunogenicity of Recombinant Vesicular Stomatitis Virus Ebola Vaccine in Healthy Adults: A Randomized Clinical Trial. *CMAJ* 189(24):E819-E827. <https://doi.org/10.1503/cmaj.170074>
- Ha S., Hu Z., Olson M.A., Lee K.H., Torrelles J.B., Chang W., et al. (2024) N-Substituted Pyrrole-Based Heterocycles as Broad-Spectrum Filoviral Entry Inhibitors. *J Med Chem* 67(12):10132-10151. <https://doi.org/10.1021/acs.jmedchem.4c00527>
- Hoenen T., Groseth A., Callison J., Takada A., Feldmann H. (2013) A Novel Ebola Virus Expressing Luciferase Allows for Rapid and Quantitative Testing of Antivirals. *Antiviral Res* 99(3):207-213. <https://doi.org/10.1016/j.antiviral.2013.05.017>
- Hoenen T., Groseth A., Feldmann H. (2012) Current Ebola Vaccines. *Expert Opin Biol Ther* 12(7):859-872. <https://doi.org/10.1517/14712598.2012.685152>
- Venkatraman N., Ndiaye B.P., Bowyer G., Wade D., Sridhar S., Wright D., et al. (2019) Safety and Immunogenicity of a Heterologous Prime-Boost Ebola Virus Vaccine Regimen in Healthy Adults in the United Kingdom and Senegal. *J Infect Dis* 219(8):1187-1197. <https://doi.org/10.1093/infdis/jiy639>
- Wang Y., Li J., Hu Y., Liang Q., Wei M., Zhu F. (2017) Ebola Vaccines in Clinical Trial: The Promising Candidates. *Hum Vaccin Immunother* 13(1):153-168. <https://doi.org/10.1080/21645515.2016.1225637>
- Zarro M., Bashlakova K., Dellisanti B., Brunone S., Villari P., De Vito C., Rosso A. (2025) Immunogenicity and Safety of Ebola Vaccines in Children: A Systematic Review and Meta-analysis. *Int J Infect Dis* 162:108171. <https://doi.org/10.1016/j.ijid.2025.108171>
- Devhare P., Desai S., Lole K. (2016) Innate Immune Responses in Human Hepatocyte-derived Cell Lines Alter Genotype 1 Hepatitis E Virus Replication Efficiencies. *Sci Rep* 6:26827. <https://doi.org/10.1038/srep26827>
- Ebola virus protein VP40 stimulates IL-12- and IL-18-dependent activation of human natural killer cells. *JCI Insight* 7(16):e158902. <https://doi.org/10.1172/jci.insight.158902>
- Falzarano D., Feldmann H. (2014) Possible Leap Ahead in Filovirus Therapeutics. *Cell Res* 24(6):647-648. <https://doi.org/10.1038/cr.2014.49>
- Kuhn J.H., Dodd L.E., Wahl-Jensen V., Radoshitzky S.R., Bavari S., Jahrling P.B. (2011) Evaluation of Perceived Threat Differences Posed by Filovirus Variants. *Biosecur Bioterror* 9(4):361-371. <https://doi.org/10.1089/bsp.2011.0051>
- Messingham K.N., Richards P.T., Fleck A., Patel R.A., Djurkovic M., Elliff J., et al. (2025) Multiple Cell Types Support Productive Infection and Dynamic Translocation of Infectious

Ebola Virus to the Surface of Human Skin. *Sci Adv* 11:eadr6140. <https://doi.org/10.1126/sciadv.adr6140>

Biffi A., Bartolomae C.C., Cesana D., Cartier N., Aubourg P., Ranzani M., et al. (2011) Lentiviral Vector Common Integration Sites in Preclinical Models and a Clinical Trial Reflect a Benign Integration Bias and Not Oncogenic Selection. *Blood* 117(20):5332-5339. <https://doi.org/10.1182/blood-2010-09-306761>

Dull T., Zufferey R., Kelly M., Mandel R.J., Nguyen M., Trono D., Naldini L. (1998) A Third-generation Lentivirus Vector with a Conditional Packaging System. *J Virol* 72(11):8463-8471. <https://doi.org/10.1128/JVI.72.11.8463-8471.1998>

Elegheert J., Behiels E., Bishop B., Scott S., Woolley R.E., Griffiths S.C., et al. (2018) Lentiviral Transduction of Mammalian Cells for Fast, Scalable and High-level Production of Soluble and Membrane Proteins. *Nat Protoc* 13(12):2991-3017. <https://doi.org/10.1038/s41596-018-0075-9>

Lin P., Lin Y., Lennon D.P., Correa D., Schlachter M., Caplan A.I. (2012) Efficient Lentiviral Transduction of Human Mesenchymal Stem Cells that Preserves Proliferation and Differentiation Capabilities. *Stem Cells Transl Med* 1(12):886-897. <https://doi.org/10.5966/sctm.2012-0086>

Melito P.L., Qiu X., Fernando L.M., deVarenes S.L., Beniac D.R., Booth T.F., Jones S.M. (2008) The Creation of Stable Cell Lines Expressing Ebola Virus Glycoproteins and the Matrix Protein VP40 and Generating Ebola Virus-like Particles Utilizing an Ecdysone Inducible Mammalian Expression System. *J Virol Methods* 148(1-2):237-243. <https://doi.org/10.1016/j.jviromet.2007.12.004>

Schambach A., Zychlinski D., Ehrnstroem B., Baum C. (2013) Biosafety Features of Lentiviral Vectors. *Hum Gene Ther* 24(2):132-142. <https://doi.org/10.1089/hum.2012.229>

Zamule S.M., Strom S.C., Omiecinski C.J. (2008) Preservation of Hepatic Phenotype in Lentiviral-transduced Primary Human Hepatocytes. *Chem Biol Interact* 173(3):179-186. <https://doi.org/10.1016/j.cbi.2008.03.015>

Bhattacharyya S. (2021) Mechanisms of Immune Evasion by Ebola Virus. In: *Adv Exp Med Biol* 1313, de Voogt P. (eds), Springer International Publishing, pp 15-22. https://doi.org/10.1007/978-3-030-67452-6_2

Roldão A., Silva A.C., Mellado M.C.M., Alves P.M., Carrondo M.J.T. (2017) Viruses and Virus-Like Particles in Biotechnology: Fundamentals and Applications. In: *Reference Module in Life Sciences*, de Voogt P. (eds), Elsevier, pp 1-15. <https://doi.org/10.1016/B978-0-12-808633-8.08046-4>